Unmanned Water Craft Identification and Adaptive Control in Low-Speed and Reversing Regions

Lukas R. S. Theisen * **Roberto Galeazzi** * **Mogens Blanke** *,**

* *Department of Electrical Engineering, Automation and Control Group, Technical University of Denmark, Kgs. Lyngby, Denmark (e-mail: {lrst, rg, mb}@elektro.dtu.dk)*
** *Centre for Autonomous Marine Operations and Systems (AMOS), Norwegian University of Science and Technology, Trondheim, Norway*

Abstract: This paper treats $\mathcal{L}_1$ adaptive hovering control of an unmanned surface vehicle in a station-keeping mode where a region of zero control authority and under-actuation are main challenges. Low-speed and reversing dynamics are identified from full scale sea trials, and parameter uncertainty is estimated. With significant parameter variation, an $\mathcal{L}_1$ adaptive controller is employed for heading control. The $\mathcal{L}_1$ family of controllers allows for several topologies and an architecture is suggested that suits heading control of a vessel, the requirements of which differ from that of previous $\mathcal{L}_1$ literature. The control design is tackled directly in discrete time to allow a fast embedded implementation in the vehicle. Analysis of robustness, tracking performance and wave disturbance response are detailed in the paper.

Keywords: $\mathcal{L}_1$ adaptive control, unmanned vehicle, system identification, discrete time control

1. INTRODUCTION

Personal water crafts (PWC) are capable of fast and agile manoeuvring and provide endurance over long distances making them suitable for complex autonomous missions. Certain missions may require station keeping as one of the use-modes, which is achieved through heading and speed control at low speed forward and aft.

The realization of station keeping for the PWC is certainly a challenge since the system is underactuated. The vehicle has an azimuth impeller equipped with an elevator, which can be used to change the vertical direction of the impeller jet. This actuation is perfect at high forward speed to execute fast manoeuvres; however at low speed the controllability of the system reduces.

Control of underactuated vehicles has received a great attention (see e.g. Pettersen and Fossen (2000); Fossen and Strand (2001); Blanke (2005); Pereira et al. (2008)), but it still is an open and interesting control problem. Fossen and Strand (2001) proposed the weather optimal heading control, where the marine craft is steered to be on a virtual circle headed towards the center. A set of model parameters were at hand for the considered vessel and a PD regulator was designed using the backstepping design methodology with the inclusion of integral action.

For the PWC there is no model readily available, and the identification of the system dynamics solely relies on full scale motion data always affected by induced oscillations in the wave frequency range. This results in significant parameter variation, which calls in for robust and adaptive control strategies.

The development of the $\mathcal{L}_1$ adaptive control theory (Hovakimyan and Cao, 2010) has allowed for design of controllers ensuring uniform closed loop transient response over a wide range of parametric uncertainties, while guaranteeing robustness and stability. Svendsen et al. (2012) took the first steps towards a fully autonomous PWC by designing and implementing two independent $\mathcal{L}_1$ adaptive controllers for cruise and steering control at medium to high speed.

This paper proposes a low speed adaptive heading controller suitable for station keeping. The architecture of the $\mathcal{L}_1$ adaptive controller is modified in order to best fit the heading control problem, and the controller is completely and directly designed in discrete time to enable fast embedded implementation in the vehicle. Robustness and performance of the proposed heading controller is analyzed w.r.t. model uncertainties and disturbances.

2. SYSTEM CONFIGURATION

The water jet vehicle is a modified Sea-Doo GTX 215 personal water craft (see Fig. 1), whose physical specifications are listed in table A.1. A radio link between the vehicle and a ground station allows remote command of three servos, which control the throttle, the azimuthal angle of the water jet, and the elevator angle of a blade constraining the angle of attack of the pressurized water stream w.r.t. the horizontal.

The elevator angle or deflection β of the blade w.r.t. the horizontal is in the interval $\beta \in [0°; 55°]$ and a deflection β corresponds to a deflection of the water jet of 2β, as illustrated in Fig. 1. Similarly the azimuth δ controls the horizontal direction of the water jet, giving a moment

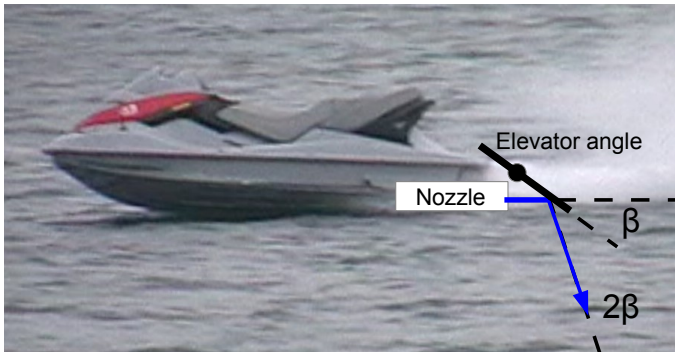

Fig. 1. PWC with deflected elevator: a deflection β causes the water jet to be deflected by an angle equal to 2β.

around the z-axis. The maximum angular deflection is $\delta_{\max} = 15°$ to each side with a rate limit of $\dot{\delta} \leq 30°/\,\mathrm{s}$.

3. PWC REVERSING DYNAMICS

For low speed operations such as station keeping where the speed is below 3 m/s the personal water craft behaves as a fully displaced vessel; hence the influence of the vertical dynamics into the manoeuvring characteristic is negligible. For larger ships it is assumed that the heave, roll and pitch are fairly small (Pettersen and Fossen, 2000). This assumption is extended to the dynamics of the water jet vehicle; however this may be true only in confined waters.

The 3 DOF surge-sway-yaw linear manoeuvring model is formulated according to (Clarke and Horn, 1997; Fossen, 2011). Let $\boldsymbol{\eta} \triangleq [N, E, \psi]^{\mathrm{T}}$ be the generalized position vector w.r.t. an Earth-fixed frame, and $\boldsymbol{\nu} \triangleq [u, v, r]^{\mathrm{T}}$ the generalized velocity vectors w.r.t. a body-fixed frame. The PWC dynamics in the horizontal plane is then given by

$$\dot{\boldsymbol{\eta}} = \mathbf{R}(\psi)\boldsymbol{\nu} \tag{1}$$

$$\mathbf{M}\dot{\boldsymbol{\nu}} + \mathbf{N}(u_0)\boldsymbol{\nu} = \boldsymbol{\tau}_c + \boldsymbol{\tau}_e \tag{2}$$

where $\mathbf{M}$ is the mass-inertia matrix including rigid-body and added mass; $\mathbf{N}(u_0)$ contains the linear contribution from the frictional and Coriolis-centripetal forces and moments evaluated at the forward speed u_0; $\boldsymbol{\tau}_c$ and $\boldsymbol{\tau}_e$ are the vectors of generalized control and environmental forces; $\mathbf{R}(\psi)$ is the rotation matrix that maps velocities from body- to the Earth-fixed frame.

Assuming that the water craft has xz-plane symmetry and that the mass distribution is even, surge can be decoupled from steering. Therefore $\mathbf{M}$ and $\mathbf{N}$ in (2) read

$$\mathbf{M} = \begin{bmatrix} m - X_{\dot{u}} & 0 & 0 \\ 0 & m - Y_{\dot{v}} & mx_g - Y_{\dot{r}} \\ 0 & mx_g - N_{\dot{r}} & I_z - N_{\dot{r}} \end{bmatrix}$$

$$\mathbf{N}(u_0) = \begin{bmatrix} -X_u & 0 & 0 \\ 0 & -Y_v & mu_0 - Y_r \\ 0 & -N_v & mx_g u_0 - N_r \end{bmatrix}$$

where m is the mass of the vehicle, I_z is the rigid body inertia around the z-axis, x_g is the horizontal coordinate of the centre of gravity w.r.t. the origin of the body-fixed manoeuvring frame (z-down), and $X_{(\cdot)}, Y_{(\cdot)}, N_{(\cdot)}$ are the hydrodynamic derivatives.

Said T the thrust force, the control input vector $\boldsymbol{\tau}_c = [\tau_{\mathrm{X}}^c, \tau_{\mathrm{Y}}^c, \tau_{\mathrm{N}}^c]^{\mathrm{T}}$ is given by

$$\boldsymbol{\tau}_c \triangleq \mathbf{b}(\delta, \beta)T = \begin{bmatrix} \cos\delta\cos(2\beta) \\ -\sin\delta\cos(2\beta) \\ L_{\mathrm{N}}\sin\delta\cos(2\beta) \end{bmatrix} T$$

$$\approx \begin{bmatrix} \cos(2\beta) \\ -\delta\cos(2\beta) \\ L_{\mathrm{N}}\delta\cos(2\beta) \end{bmatrix} T \tag{3}$$

as the azimuthal angle $|\delta| \leq 15°$; hence $\sin\delta$ and $\cos\delta$ are replaced by their first order approximation. In (3) L_{N} is the x-distance from the center of buoyancy to the nozzle head. Equation (3) shows the effect of the elevator deflection on the manoeuvring of the PWC:

- $0 < \beta < \pi/4$ causes a forward thrust force from the impeller
- for $\pi/4 < \beta < \beta_{\max}$ the thrust changes sign and causes a reversing thrust
- $\beta = \pi/4$ is a singular configuration in the controllability space since the input vector $\mathbf{b}(\delta, \beta)$ is zero

The availability of only the motion data gathered during full scale sea trials obviously precludes the possibility of identifying the coefficients of the matrices $\mathbf{M}$ and $\mathbf{N}(u_0)$. Therefore the identification of the low-speed reversing dynamics relies on linear output models parametrized in terms of time constants and gains. Hence the action of environmental forces/moments $\boldsymbol{\tau}_e$ is modelled as output disturbances.

3.1 Low-Speed Surge Dynamics Identification

The decoupled surge dynamics reads

$$\dot{u}(t) = \frac{-X_u}{m - X_{\dot{u}}}u(t) + f(h,t)\cos(2\beta(t)) \;, \tag{4}$$

where $f(h,t)$ is the body x component of the thrust. The throttle handle h has been constrained to the constant value $\bar{h} = 1$, it is therefore assumed $f(h,t) = \bar{f}$ is constant. Equation (4) can be rewritten in transfer function form as

$$u(s) = \frac{K_u}{T_u s + 1} g_\beta(s) \;, \tag{5}$$

where $g_\beta(s)$ is the Laplace transform of $\cos(2\beta(t))$; $K_u \triangleq \bar{f}$ is the steady state surge gain for a constant β; $T_u \triangleq (X_u/(m - X_{\dot{u}}))^{-1}$ is the time constant.

The parameters K_u and T_u are estimated from full scale data collected in response to elevator steps. The identified model is

$$\mathcal{M}_{u,g}: \quad u(s) = \frac{2.46}{5.58s + 1} g_\beta(s) \tag{6}$$

whose fit to the data set in identification is 92.3%, and in validation is 85.4%. Figure 2 shows the comparison between the full scale data and the surge model $\mathcal{M}_{u,g}$ for the identification and validation data sets.

3.2 Low-Speed Steering Dynamics Identification

The linear output yaw model associated to (2) is

$$r(s) = H_{nom}(s)\delta(s) + r_w(s) \;, \quad H_{nom} = \frac{\mathcal{K}_n}{\mathcal{T}_n s + 1} \tag{7}$$

which is the first order Nomoto model (Nomoto et al., 1957) affected by external disturbances, where

$$\mathcal{K}_n = -N_\delta \mathcal{D}_n \;, \; \mathcal{T}_n = (I_z - N_{\dot{r}})\mathcal{D}_n$$

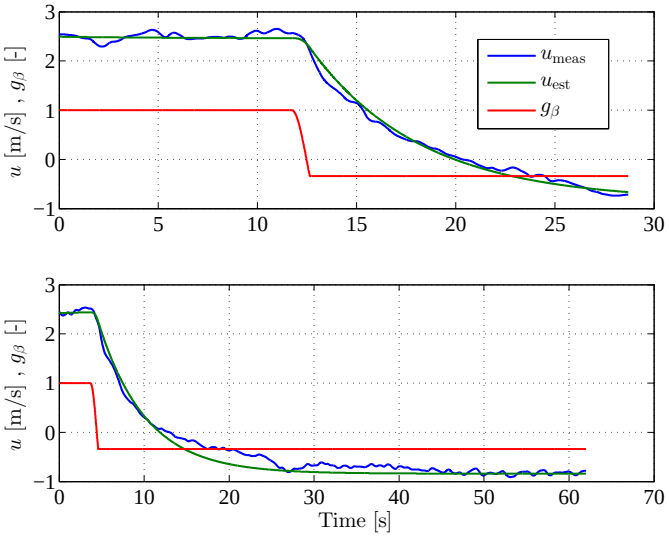

Fig. 2. Identification and validation of the surge dynamics from elevator steps: (top) model $\mathcal{M}_1$ identified for $\psi \approx 260°$; (bottom) model $\mathcal{M}_1$ validated for $\psi \approx 0°$.

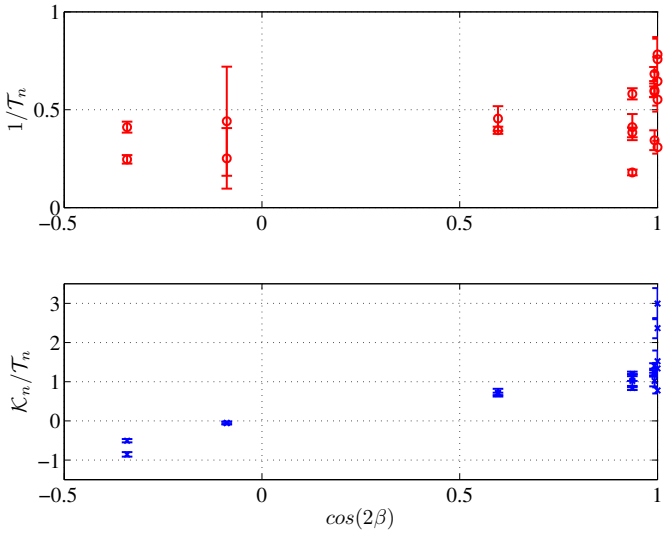

Fig. 3. Estimated parameters of the first order Nomoto model with $\pm 1\sigma$ uncertainty.

with $\mathcal{D}_n = ((mx_g - Y_{\dot{r}})u_0 - N_r)^{-1}$. The wave disturbance $r_w(s)$ is modelled as the output of a second order filter driven by white noise $e_w(t)$

$$r_w(s) = \frac{\kappa_w s}{s^2 + 2\lambda_w \omega_w s + \omega_w^2} e_w(s) \; . \tag{8}$$

The model (7) is used for identifying the low-speed manoeuvring dynamics of the PWC. The wave model (8) is introduced to take into account the presence of wave motion in the experimental data sets. The identification of the yaw dynamics is performed by using full scale motion data collected during 19 circular tests at different elevator angles β. The Box-Jenkins model structure (Box and Jenkins, 1970) is used to represent the dynamics (7), and the model's parameters are estimated using the prediction error method (Ljung, 1999).

Figure 3 shows the estimated Nomoto model parameters with $\pm 1\sigma$ uncertainty. The estimates have generally a very low uncertainty, except for the two sea trials performed at $\beta \approx \pi/4$ when the vehicle is close to the controllability singularity. The estimate of the pole $1/\mathcal{T}_n$ is not very consistent, i.e. experiments repeated at the same elevator angle do not provide similar values, especially for $\beta \approx 0$. This may address the influence of the low frequency component of the wave motion on the estimation of the PWC dynamics. Instead the estimate of the gain $\mathcal{K}_n/\mathcal{T}_n$ is more robust, with the presence of only two outliers for $\beta = 0$. Figure 3 also shows the sign dependency of the input gain on the deflection of the elevator. This poses an important issue for the design of adaptive controllers, which requires the definition of a new control input, as shown in Sec. 4.1.

Standard methods of system identification have been used to assess the validity of the identified Nomoto models, such as parameter's sign test and residual whiteness. The analysis of these two indicators clearly addressed the under-parametrization of the chosen model structure with respect to the dynamics present on the full scale data. However, since low complexity models are sought, and the first order Nomoto model certainly catches the low frequency manoeuvring characteristics of the vehicle, it was deemed to be sufficient.

4. TOWARDS STATION KEEPING

In the design towards a station keeping system, a heading controller is an important aspect. This section presents a step towards station keeping in projecting a discrete time $\mathcal{L}_1$ adaptive heading controller for the PWC. Surge control can be performed using e.g. (Fossen and Strand, 2001; Pettersen and Fossen, 2000), and it is not be considered further in this paper.

4.1 Forced Yaw Acceleration

A new control input is defined as the forced yaw acceleration

$$\bar{a}_{\text{N}}^c(\beta, \delta) \triangleq \frac{-N_\delta(\beta)}{I_z - N_{\dot{r}}} \delta \; , \tag{9}$$

where $N_\delta(\beta) = TL_{\text{N}} \cos(2\beta)$ is a function of the elevator angle. By including N_δ in the new control input the sign of the input gain is preserved. This guarantees that the input gain does not switch sign during system's operation, which is needed in order to design the adaptive controller.

Figure 4 shows the dependency of the physical torque gain N_δ on the elevator deflection. N_δ has been estimated by

$$\mathcal{D}_n = \frac{\mathcal{T}_n}{I_z - N_{\dot{r}}} \Rightarrow N_\delta = \frac{\mathcal{K}_n}{\mathcal{D}_n} \tag{10}$$

where I_z has been computed by considering the PWC as a rigid rod with most of the mass placed at the center, and the added inertia $N_{\dot{r}} < 0$ has been assumed constant and equal to 80% of I_z ($I_z - N_{\dot{r}} \approx 460\,\text{kg}\,\text{m}^2$).

The indirect estimate of N_δ is strongly affected by the inconsistency in the estimate of $\mathcal{T}_n$ for values of β close to zero. Hence the values of N_δ are scattered, determining an uncertainty in the magnitude of $\bar{a}_{\text{N}}^c$. This uncertainty is modelled as

$$a_{\text{N}}^c(\beta, \delta) = \omega \bar{a}_{\text{N}}^c(\beta, \delta), \quad \omega \in [\omega_{\min}, \omega_{\max}] \tag{11}$$

where ω is an uncertain input gain and $\omega_{\max} > \omega_{\min} > 0$.

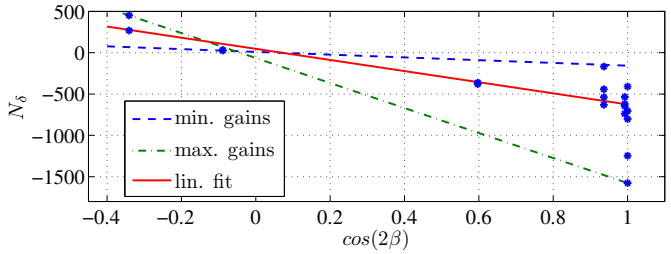

Fig. 4. Torque gain N_δ as function of elevator angle β. Min and max gains are estimated using linear approximation.

4.2 Discrete Time $\mathcal{L}_1$ Adaptive Heading Controller

The control objective is to regulate the vehicle heading as desired, despite the presence of environmental disturbances and unknown nonlinear manoeuvring characteristics. However control effort should be limited in the wave frequencies range to reduce wear and tear of the actuator. This is fulfilled through a two step design: first a baseline PD regulator is dimensioned for the nominal heading dynamics; then the feedback loop is augmented with an $\mathcal{L}_1$ adaptive controller, which guarantees scalable transient performance in presence of changes in system parameters. The heading controller is designed for operation at the elevator angles $\beta \in \{0°; 55°\}$ and for a forward speed $U < 3\,\mathrm{m/s}$.

The proposed architecture for the $\mathcal{L}_1$ adaptive controller exploits the physical correlation between heading angle and turning rate to reduce the complexity (order of the system) of the state predictor and the adaptation law. Moreover, since the ultimate objective is the embedded implementation of the station keeping controller in the real vehicle, the design of the $\mathcal{L}_1$ augmented PD heading controller is undertaken in discrete time.

For controller design the steering dynamics (7) is reformulated in discrete time state space form in terms of the heading error $\psi_e(k) = \psi_{ref}(k) - \psi(k)$, $(\psi_e \in]-\pi;\pi])$. Let $\mathbf{x} \triangleq [\psi_e, r]^{\mathrm{T}}$ be the state vector, $u = \bar{a}_{\mathrm{N}}^{\mathrm{c}}$ the control input, and r_w the wave disturbance. Then the heading error dynamics reads

$$\mathbf{x}(k+1) = \mathbf{F}\mathbf{x}(k) + \mathbf{g}(\omega u(k) + f(k)) + \mathbf{e}r_w(k) \quad (12)$$

$$\mathbf{y}(k) = \mathbf{C}\mathbf{x}(k) + \mathbf{d}r_w(k) \quad (13)$$

where

$$\mathbf{F} = \begin{bmatrix} 1 & \mathcal{T}_n\left(e^{-\frac{T_s}{\mathcal{T}_n}} - 1\right) \\ 0 & e^{-\frac{T_s}{\mathcal{T}_n}} \end{bmatrix}, \quad \mathbf{g} = \begin{bmatrix} \mathcal{T}_n^2\left(1 - e^{-\frac{T_s}{\mathcal{T}_n}} - \frac{T_s}{\mathcal{T}_n}\right) \\ \mathcal{T}_n\left(1 - e^{-\frac{T_s}{\mathcal{T}_n}}\right) \end{bmatrix}$$

$$\mathbf{e} = \begin{bmatrix} T_s \\ 0 \end{bmatrix}, \quad \mathbf{C} = \begin{bmatrix} 1 & 0 \\ 0 & 1 \end{bmatrix}, \quad \mathbf{d} = \begin{bmatrix} 0 \\ 1 \end{bmatrix},$$

T_s is the sampling time, and $f(k)$ is an unknown nonlinear function that represents the unmodelled cross-couplings with sway and surge. The control signal u is designed as the sum of two contributions

$$u(k) = u_{\mathrm{PD}}(k) + u_{\mathrm{AD}}(k)\,, \quad (14)$$

where u_{PD} is the command of the PD regulator, and u_{AD} is the command of the $\mathcal{L}_1$ adaptive controller.

Baseline PD Regulator The baseline PD regulator is

$$u_{\mathrm{PD}}(k) = -\sum_{i=0}^{k} h_f(k-i)\left(k_P\psi_e(i) + k_D r(i)\right) \quad (15)$$

where k_P and k_D are the proportional and derivative gains, and $h_f(k)$ is the unit pulse response of the wavefilter

$$H_f(z) = \frac{k_H(z^2 + 2\zeta_f\omega_{f_1}z + \omega_{f_1}^2)}{\left(z - e^{-\alpha_f\omega_{f_1}T_s}\right)\left(z - e^{-\frac{\omega_{f_1}T_s}{\alpha_f}}\right)\left(z - e^{-\omega_{f_2}T_s}\right)}\,,$$

which limits the control actuation in response to high frequency wave induced motion.

$\mathcal{L}_1$ Adaptive PD Augmentation Due to the physical correlation between heading angle and turning rate, the architecture of the $\mathcal{L}_1$ adaptive controller is based only on the turning rate dynamics. Actually it is only the turning rate dynamics that can be uncertain, and that is directly affected by environmental disturbances, as shown in (1)-(2). Hence the yaw dynamics (12)-(13) is reduced to

$$r(k) = f_{22}r(k) + g_2(\omega(u_{\mathrm{PD}}(k) + u_{\mathrm{AD}}(k)) + f(k) + a_{\mathrm{W}}^{e}(k)) \quad (16)$$

$$y_{\mathcal{L}_1}(k) = r(k) \quad (17)$$

where $a_{\mathrm{W}}^{e}(k)$ is the yaw rate induced acceleration due to wind and waves.

The proposed $\mathcal{L}_1$ architecture springs from the design proposed in Xargay et al. (2010) and uses the piecewise constant adaptive laws proposed in Cao and Hovakimyan (2009). However, to the authors' knowledge this is the first attempt to tackle the design of the $\mathcal{L}_1$ adaptive controller directly in discrete time. The proposed architecture results in

State predictor The state predictor is based on the reference model (16) and represents the desired closed loop dynamics

$$\hat{r}(k+1) = f_{22}\hat{r}(k) + g_2(\omega_0 u_{\mathrm{PD}}(k) + u_{\mathrm{AD}}(k) + \hat{\sigma}(k)) \quad (18)$$

where $\hat{\sigma}$ is the estimate of the model uncertainty, and ω_0 is the nominal value of the uncertain gain ω.

Adaptation law The estimate of the unmodelled dynamics relies on the prediction error $\tilde{r}(k) = \hat{r}(k) - r(k)$ as

$$\hat{\sigma}(k) = -g_2^{-1}f_{22}\tilde{r}(k) = -K_\sigma\tilde{r}(k) \quad (19)$$

where K_σ is the adaptation gain, which is clearly a function of the sampling time T_s and the system parameters.

Control law The adaptive control signal u_{AD} is a lowpass filtering of the adaptive estimate, which ensures tracking up to a chosen bandwidth

$$u_{\mathrm{AD}}(z) \triangleq -kD(z)\hat{\eta}(z) \quad (20)$$

where k is the feedback gain, $D(z)$ is a lowpass filter containing a pure integrator, and $\hat{\eta}(z)$ is the $\mathcal{Z}$-transform of

$$\hat{\eta}(k) = (\omega_0 u(k) + \hat{\sigma}(k))\,. \quad (21)$$

By choosing the lowpass filter as

$$D(z) = \frac{k_1(z + z_1)}{(z-1)(z-p_1)} \quad (22)$$

and assuming $\omega_0 = 1$ the control law then reduces to

$$u(z) = -C(z)\hat{\sigma}(z) \quad (23)$$

$$C(z) = \frac{kk_1(z + z_1)}{z^2 + (kk_1 - p_1 - 1)z + p_1 + kk_1z_1} \quad (24)$$

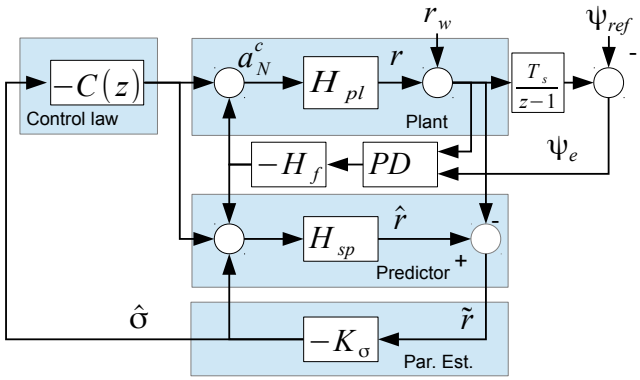

Fig. 5. The discrete time $\mathcal{L}_1$ adaptive heading controller architecture with the baseline PD regulator.

4.3 Robustness Analysis of $\mathcal{L}_1$ Adaptive Controller

The bandwidth of the filter $C(z)$ sets a clear trade-off between the adaptation to unmodelled dynamics and the sensitivity of the control signal to wave disturbances. The robustness properties of the adaptive controller are investigated by a frequency analysis showing the system performance in response to changes in the nominal plant.

For the calculations the plant is given a multiplicative uncertainty ω, and it is converted to discrete time along with the state predictor

$$H_{pl}(z) = \mathcal{Z}\{\omega/(\mathcal{T}_n s + 1)\} \quad (25)$$
$$H_{sp}(z) = \mathcal{Z}\{1/(\mathcal{T}_n s + 1)\} \quad (26)$$

The discrete time $\mathcal{L}_1$ adaptive controller is shown in Fig. 5. The relevant transfer functions, namely from reference to heading and from disturbance to forced yaw acceleration, are calculated to be

$$H_{\psi\psi_{ref}}(z) = \frac{H_{pl}T_s k_P H_f(1 + H_{sp}K_\sigma)}{d(z)} \quad (27)$$

$$H_{a^c_N r_w}(z) = \frac{1}{d(z)}(-CK_\sigma z - CK_\sigma + H_f k_D z - H_f k_D + H_f k_D H_{sp} K_\sigma z - H_f k_D H_{sp} K_\sigma + T_s H_f k_P + T_s H_f k_P H_{sp} K_\sigma) \quad (28)$$

where

$$d(z) = (z - 1 + H_{sp}K_\sigma z - CH_{sp}K_\sigma z + CH_{sp}K_\sigma - H_{sp}K_\sigma + H_{pl}T_s k_P H_f + H_{pl}k_D H_f z - H_{pl}k_D H_f + H_{pl}K_\sigma C z - H_{pl}K_\sigma C + H_{sp}K_\sigma H_{pl}T_s k_P H_f + H_{sp}K_\sigma H_{pl}k_D H_f z - H_{sp}K_\sigma H_{pl}k_D H_f) \quad (29)$$

$H_{\psi\psi_{ref}}(z)$ and $H_{a^c_N r_w}(z)$ are evaluated in response to a large plant variation ($\omega = 3$). By increasing the bandwidth of $C(z)$ a better adaptation to the reference model in presence of uncertainties is achieved; however this comes at the cost of a larger gain from disturbance to control signal, as shown in Fig. 6. The bandwidth of $C(z)$ is hence chosen such that $H_{a^c_N r_w}(z)$ has a sufficiently small magnitude in the range of frequencies where the wave disturbances is active ($\approx 3 \div 6$ rad/s). This gives an upper limitation for the bandwidth of $C(z)$ and thereby the adaptation properties. The chosen $C(z)$ has the parameters given in table B.1.

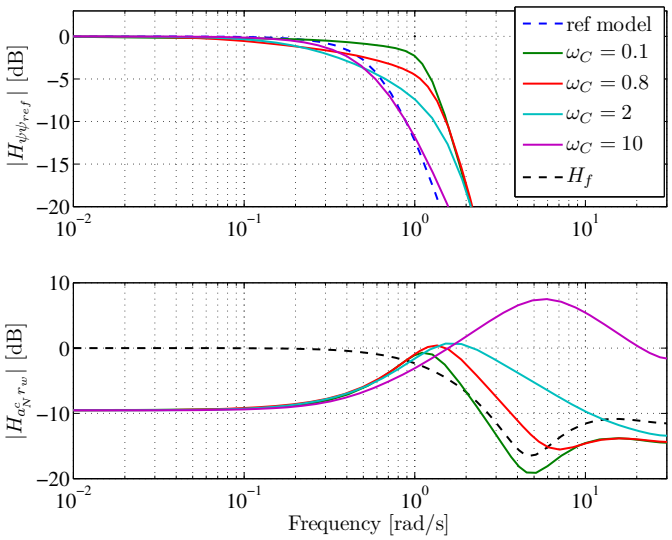

Fig. 6. Robustness analysis: the bandwidth of $C(z)$ gives a trade-off between adaptation to system's changes and undesired actuation in response to wave motion.

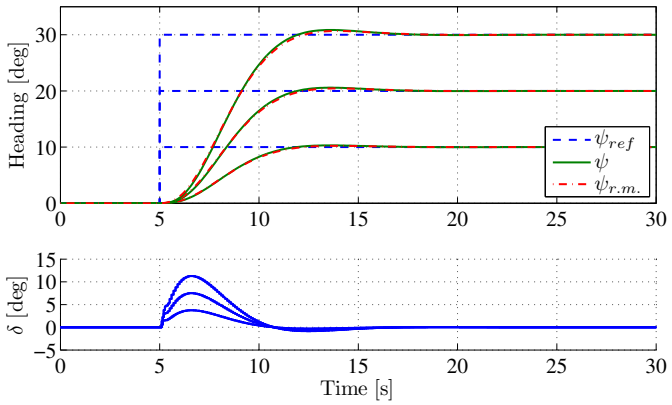

Fig. 7. Step responses showing the scalability of the adaptive controller.

5. PERFORMANCE ASSESSMENT

The desired closed loop step response should have an overshoot less than 5%, and a rise time of approximately 4.2 seconds. Suitable parameters for the baseline controller achieving these requirements are listed in table B.1.

The performance of heading controller is first assessed by step changes. Figure 7 shows the scalability of the transient response of the $\mathcal{L}_1$ adaptive heading controller. Figure 8 shows the performance of the PWC during an elevator step simulation. The elevator steps and causes the surge to change sign and thereby the input gain.

Last the $\mathcal{L}_1$ adaptive heading controller is tested against wave disturbances, as shown in Fig. 9. As expected the controller limits the use of control authority to counteract the wave motion, while regulating the heading around the desired value.

6. CONCLUSIONS

This paper presented a solution towards station keeping of an unmanned personal water craft, based on a dis-

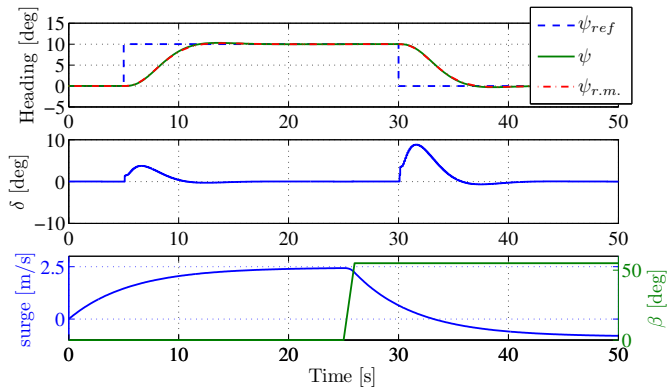

Fig. 8. Heading reference steps under changing surge.

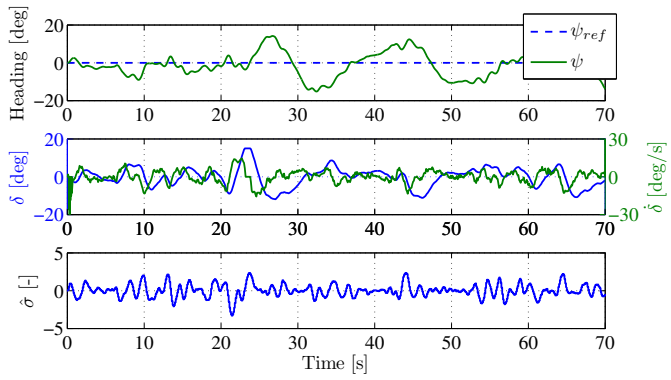

Fig. 9. Heading control in waves: the desired heading is maintained without overloading the actuator.

crete time $\mathcal{L}_1$ adaptive heading controller. First, a steering model for the PWC in low-speed and reversing regions was identified based on full scale motion data. The identified model showed large parameter variations in response to similar operational conditions. A robust adaptive heading controller was then designed, which combines a baseline PD regulator with a discrete time $\mathcal{L}_1$ adaptive controller. The proposed control architecture exploits the physical correlation between heading angle and turning rate to reduce complexity of the state predictor and the adaptation law. A robustness analysis was carried out, which showed the trade-off between adaptation and disturbance rejection properties. Simulation results confirmed the validity of the proposed heading controller for station keeping purposes.

ACKNOWLEDGEMENTS

The collaboration with the Naval Drone Section of the Danish Navy is gratefully acknowledged. Enthusiastic support from Leif Kurt Hevang and from Jens Adrian, leader of the research group, is also gratefully appreciated.

REFERENCES

Blanke, M. (2005). Diagnosis and fault-tolerant control for ship station keeping. In *Proc. 13th Mediterranean Conference on Control and Automation.*

Box, G.E.P. and Jenkins, G.M. (1970). *Time Series Analysis, Forecasting and Control.* Holden-Day.

Cao, C. and Hovakimyan, N. (2009). $\mathcal{L}_1$ adaptive output-feedback controller for non-strictly positive real reference systems: Missile longitudinal autopilot design. *AIAA Journal of Guidance, Control, and Dynamics*, 32(3), 717–726.

Clarke, D. and Horn, J.R. (1997). Estimation of hydrodynamic derivatives. In *Proc* 11^{th} *Ship Control Systems Symposium (*11^{th} *SCSS)*, volume 2, 275–289.

Fossen, T.I. (2011). *Handbook of Marine Craft Hydrodynamics and Motion Control.* John Wiley & Sons.

Fossen, T.I. and Strand, J.P. (2001). Nonlinear passive weather optimal positioning control (wopc) system for ships and rigs: experimental results. *Automatica*, 37(5), 701–715.

Hovakimyan, N. and Cao, C. (2010). *L1 Adaptive Control Theory: Guaranteed Robustness with Fast Adaptation.* SIAM Soc. for Industrial and Applied Mathematics.

Ljung, L. (1999). *System Identification: Theory for the User.* Prentice Hall, second edition.

Nomoto, K., Taguchi, T., Honda, K., and Hirano, S. (1957). On the steering qualities of ships. *International Shipbuilding Progress*, 4, 354–370.

Pereira, A., Das, J., and Sukhatme, G.S. (2008). An experimental study of station keeping on an underactuated asv. In *Proc Int Conf on Intelligent Robots and Systems*, 3164–3171. IEEE.

Pettersen, K.Y. and Fossen, T.I. (2000). Underactuated dynamic positioning of a ship - experimental results. *IEEE Tra. on Control Systems Technology (TCST)*, 8(5), 856–863.

Svendsen, C.H., Holck, N.O., Galeazzi, R., and Blanke, M. (2012). $\mathcal{L}_1$ adaptive manoeuvring control of unmanned high-speed water craft. In *Proc. 9th IFAC Conf. on Manoevring and Control of Marine Craft (MCMC'2012).*

Xargay, E., Hovakimyan, N., and Cao, C. (2010). $\mathcal{L}_1$ adaptive controller for multi-input multi-output ssystem in the presence of nonlinear unmatched uncertainties. In *Proceedings of the 2010 American Control Conference.*

Appendix A. WATERJET CRAFT PARAMETERS

The parameters of the system are listed in table A.1.

Table A.1. Sea-Doo GTX 215 specifications

Quantity	Measure
Nominal length (measured)	3.25 m
Width	1.22 m
Dry weight	388 kg
Engine max power	158 kW

Appendix B. CONTROL SYSTEM PARAMETERS

The parameters of the system are listed in table B.1.

Table B.1. System Parameters

Parameter	Value	Unit	Parameter	Value	Unit
$\mathcal{K}_n$	1.00	-	$\mathcal{T}_n$	1.67	s
ω_{f1}	4.5	rad/s	ω_{f2}	7.0	rad/s
α_f	0.3	-	ζ_f	0.3	-
ω_0	1	-	T_s	0.1	s
k	0.16	-	p_1	0.938	-
k_1	$4.894 \cdot 10^{-3}$	-	k_D	0.7	-
k_P	0.5	-	k_H	0.2754	-